

## **The effect of specific chloride adsorption on the electrochemical behavior of ultrathin Pd films deposited on Pt(111) in acid solution**

M. Arenz<sup>a\*</sup>, V. Stamenkovic<sup>b</sup>, T.J. Schmidt<sup>c</sup>, K. Wandelt<sup>a</sup>, P.N. Ross<sup>b</sup>, N.M. Markovic<sup>b\*</sup>

<sup>a</sup> Institut für Physikalische und Theoretische Chemie, Universität Bonn, Wegelerstr.12, D-53115 Bonn, Germany

<sup>b</sup> Materials Science Division, Lawrence Berkeley National Laboratory, University of California, Berkeley, CA 94720 USA

<sup>c</sup> present address: Paul-Scherrer-Institut, CH-5232 Villingen-PSI, Switzerland

\* corresponding authors: [arenz@thch.uni-bonn.de](mailto:arenz@thch.uni-bonn.de), [nmmarkovic@lbl.gov](mailto:nmmarkovic@lbl.gov)

### **Abstract**

The electrochemical behavior of thin Pd films supported on a Pt(111) electrode is investigated by cyclic voltammetry (CV) and in-situ Fourier transform infrared (FTIR) spectroscopy. It is demonstrated that in perchloric acid solution underpotential deposition of hydrogen ( $H_{upd}$ ) and hydroxyl adsorption ( $OH_{ad}$ ) is in strong competition with the adsorption of  $Cl^-$  anions, the latter being present as a trace impurity in  $HClO_4$ . The interaction of  $Cl^-$  with Pd is rather strong, controlling the adsorption of  $H_{upd}$  and  $OH_{ad}$  as well as the kinetic rate of CO oxidation. The microscopic insight (the binding sites) of the adsorbed CO ( $CO_{ad}$ ) and the rate of CO oxidation (established from  $CO_2$  production) on Pt(111) modified with a (sub)monolayer of Pd is elucidated by means of Fourier infrared

(FTIR) spectroscopy. The appearance of both the characteristic Pt(111)-CO<sub>ad</sub> and Pt(111)1 ML Pd-CO<sub>ad</sub> stretching bands on a Pt(111) surface covered by 0.5 ML Pd confirms previous findings that the Pd atoms agglomerate into islands and that the bare Pt areas and the Pd islands behave according to their own surface chemistry. The systematic increase of the Pd surface coverage results in a gradual change in the catalytic properties of Pt(111)-xPd electrodes towards CO oxidation, from those characteristic of bare Pt(111) to those which are characteristic for Pt(111) covered with 1 ML of Pd.

Keywords: Electrochemical methods, Reflection spectroscopy, Metal-electrolyte interfaces, Adsorption kinetics, Carbon monoxide, Platinum, Palladium

## 1. Introduction

During the last decade there has been a substantial progress in the field of surface (electro)chemistry on bimetallic surfaces which are created by deposition of ultrathin metal films on well-characterized surfaces. After the successful UHV studies [1-3] and complementary quantum-chemical calculations [4-6], the adsorption and catalytic properties of pseudomorphic Pd films supported on Pt [7-11] and Au [12-15] single crystals has also received considerable attention in the field of surface electrochemistry. For example, the morphology and stability of Pd films on Pt(111) were examined by utilizing in-situ surface x-ray diffraction [11] and FTIR measurements [16, 17]. SXS studies demonstrated that both UHV and electrochemically deposited films are pseudomorphic, i.e. the position of the Pd atoms is in registry with the underlying substrate. The palladium (sub)monolayer films are rather stable in the potential region between hydrogen evolution and oxide formation, showing no sign of hydrogen *absorption*, characteristic for bulk Pd and also observed for 3D Pd islands deposited on Pt(hkl) with  $\Theta_{\text{Pd}} > 1 \text{ ML}$  [18]. FTIR characterization of  $\text{CO}_{\text{ad}}$  on Pt(111) modified with  $0 \text{ ML} < \Theta_{\text{Pd}} < 1 \text{ ML}$  was used as an indirect probe in order to establish whether Pd forms 2D island or whether the Pd atoms are dispersed on the surface much more randomly, as seen for example for the deposition of Bi on transition metals [19]. The fact that three different C-O stretching bands, corresponding to  $\text{CO}_{\text{ad}}$  on Pd and on the bare Pt substrate, are observed on a Pt(111) electrode partially covered by Pd, indirectly suggested that Pd atoms form islands and that Pt and Pd exhibit their own individual surface chemistry [16, 17]. Very recently, it has been proposed that the kinetics of CO oxidation on Pt(hkl) is not governed only by the surface concentration of  $\text{CO}_{\text{ad}}$  and  $\text{OH}_{\text{ad}}$  species, but is also

strongly affected by the delicate balance between the coverage of  $\text{CO}_{\text{ad}}$ ,  $\text{OH}_{\text{ad}}$  and anions from the respective supporting electrolyte [20].

The objective of the present paper is to elucidate the relationship between the structure and the composition of the  $\text{Pt}(111)\text{-xPd}$  surface and the kinetics of CO oxidation in perchloric acid solution. It will be shown that the strong interaction between Pd and  $\text{Cl}^-$  controls both the adsorption of  $\text{H}_{\text{upd}}$  and  $\text{OH}_{\text{ad}}$  as well as the kinetic rate of CO oxidation. FTIR measurements confirm that the Pd atoms coalesce into islands on  $\text{Pt}(111)$ , forming a bimetallic surface in which the Pt and Pd patches retain their own characteristic surface electrochemistry. It will be shown that the systematic increase of the Pd surface coverage results in an increasing inhibition of CO oxidation, suggesting that Pt atoms are more active for CO oxidation than Pd atoms. This finding is consistent with a stronger Pd-Cl than Pt-Cl interaction, e.g.,  $\text{Cl}_{\text{ad}}$  acts primarily as a site blocking inhibitor for  $\text{OH}_{\text{ad}}$  adsorption on Pd sites.

## 2. Experimental

### 2.1 Electrochemical measurements

The pretreatment and mounting of the  $\text{Pt}(111)$  single crystal in a rotating disk electrode configuration was fully described previously [21]. In short, following crystal cleaning by flame annealing in a hydrogen flame and cooling in a mild argon stream the crystal was protected by a drop of ultra pure water, transferred to and mounted into the disk position of an insertable ring-disk electrode (RDE) assembly (*Pine Instruments*). Subsequently, the electrode was transferred into the electrochemical cell. For the electrochemical deposition of palladium the clean, flame annealed  $\text{Pt}(111)$  sample was subjected to a potential cycling between  $0.05 < E < 0.9$  V in a  $0.05\text{ M H}_2\text{SO}_4 + 5 \cdot 10^{-6}\text{ M}$

PdO solution with a sweep rate of 50 mV/s. The amount of Pd deposited was controlled by monitoring the continuous change of the voltammetric features from those characteristic of bare Pt(111) to those of a pseudomorphic monolayer of palladium. Since the onset of 3-D palladium growth, indicated by a second peak at about 0.3 V in the cyclic voltammogram [20], may actually start shortly before the completion of the pseudomorphic monolayer, the formation of the peak at 0.3 V during palladium deposition was avoided. The palladium coverage, indicated in the text, is calculated using a calibration curve established by plotting the charge densities in the  $H_{upd}$ -region of the CV's of UHV-prepared Pt(111)-xPd surfaces against the Pd coverage  $x$  as determined by low energy ion scattering (LEIS) [17]. After the electrochemical Pd deposition, the electrode was rinsed with ultra pure water and transferred either into the *in-situ* FTIR cell or to a thermostated standard three compartment electrochemical cell for recording the cyclic voltammograms, both containing 0.1 M  $HClO_4$  solution. For the electrochemical cell a circulating constant temperature bath (*Fischer Isotemp Circulator*) maintained the temperature of the electrolyte constant within  $\pm 0.5$  K.

The acid solutions were prepared from concentrated sulfuric acid (*Baker Ultrex*) and concentrated perchloric acid (*EM Science Suprapure*), respectively, using triply pyrodistilled water. Prior to each experiment all solutions were deaerated by purging with argon (Air Products 5N5 purity). The reference electrode for the electrochemical cells was a saturated calomel electrode (SCE) separated from the working electrode compartment by a closed electrolyte bridge in order to avoid chloride contamination. All potentials shown in the text, however, refer to the reversible hydrogen electrode in the

same solution, calibrated from the reversible potential for the hydrogen evolution/oxidation reaction.

## 2.2 FTIR measurements

For the in-situ FTIR measurements a Nicolet Nexus 670 spectrometer was available with a nitrogen cooled MCT detector. All IR measurements were performed in a spectroelectrochemical glass cell designed for an external reflection mode in a thin layer configuration. The cell is coupled at its bottom with a  $\text{CaF}_2$  prism beveled at  $60^\circ$  from the surface normal. Prior to each measurement, a cyclic voltammogram was recorded in order to check the cleanliness of the electrode surface. Subsequently the solution was saturated with CO (Spectra Gases N4.5) for at least 3 min. holding the electrode potential at 0.05 V. For the CO oxidation measurements in argon saturated perchloric acid at first CO was adsorbed by purging the solution for 5 minutes with CO and subsequently for 20 minutes with argon, before pressing the sample onto the prism. The spectra were recorded with a resolution of  $8 \text{ cm}^{-1}$ . All measurements were performed using p-polarized light. In order to obtain a single beam spectrum 100 scans were collected at each potential resulting in a recording time of 50 s. Absorbance spectra were calculated as the ratio  $-\log(R/R_0)$  where  $R$  and  $R_0$  are the reflectance values corresponding to the sample and reference spectra, respectively. Reference spectra were recorded either at 1.0 V, where  $\text{CO}_{\text{ad}}$  is completely oxidized, or at 0.05 V before the onset of  $\text{CO}_{\text{ad}}$  oxidation. The reference potential in the spectroelectrochemical cell was controlled by a reversible hydrogen electrode (RHE).

## 3. Results and discussion

### 3.1 Cyclic voltammetry

In Figure 1a the cyclic voltammogram of bare Pt(111) in perchloric acid solution is compared to the voltammograms of two Pt(111)-xPd electrodes (with  $x \approx 0.15$  and  $x \approx 1$ , respectively) in order to establish how the systematic increase of the Pd surface coverage modifies the voltammetric profiles of Pt(111). The CV of bare Pt(111) exhibits three characteristic potential regions: the hydrogen underpotential deposition region ( $H_{\text{upd}}$ ,  $0 < E < 0.375$  V) is followed first by the double-layer potential region ( $0.375 < E < 0.6$  V) and then by the so-called “butterfly” feature ( $0.6 < E < 0.85$  V). There remains some disagreement over the identity of the processes producing the butterfly feature in perchloric acid, particularly the sharp peak near 0.8 V. In previous work from this laboratory [22,23], we have suggested the primary process is the formation of adsorbed OH, co-adsorbed with a small amount of chloride (present as an impurity in perchloric acid at a concentration of at least  $10^{-7}$  M in even the most meticulously prepared electrolyte). Ito and co-workers [24] suggested the OH was co-adsorbed with specifically adsorbed perchlorate anion, not chloride. Based on Monte Carlo simulations, Koper and co-workers suggested the sharp peak is produced by an order-disorder transition in the adsorbed OH. We note here, as we have done before [25], that for the butterfly feature in alkaline solution, where there is neither perchlorate nor chloride anion, there is no sharp peak and the total charge is as high or higher than in perchloric acid. It seems to us that the sharp peak may indeed be associated with an order-disorder transition, but not involving OH alone, but OH with a co-adsorbed anion, most probably (in our opinion) chloride. We shall come back to this issue of chloride in the perchloric acid in discussing the results with Pd modified surfaces.

Figure 1 shows that the deposition of Pd on Pt(111) produces significant changes in the cyclic voltammogram. A close inspection of Figure 1 reveals that there are three characteristics in the voltammetric profiles that demonstrate the effect of Pd. The first is an increase of the charge in the  $H_{upd}$  region with an increase of the Pd surface coverage, presumably due to a stronger Pt(111)-Pd- $H_{upd}$  interaction compared to the Pt(111)- $H_{upd}$  interaction. As shown in Figure 1b, the  $H_{upd}$  charge increases from about  $(161 \pm 5) \mu C/cm^2$  for bare Pt(111) to a value of  $(240 \pm 5) \mu C/cm^2$  for a full monolayer of Pd on Pt(111) (as a guide for the eye a dashed line is included to Figure 1b anticipating a linear dependency). These charges correspond to hydrogen coverages of  $(0.67 \pm 0.02) \text{ ML}$  and  $(1.00 \pm 0.02) \text{ ML}$ , respectively (for any adsorbate, 1ML is defined as one monovalent molecule/adatom adsorbed per Pt surface atom, or  $1.5 \times 10^{15} \text{ molecules/cm}^2$ , which is equivalent to  $240 \mu C/cm^2$ ). This observation has been reported previously also for  $H_{upd}$  in sulfuric acid [10] and alkaline [17] solutions. The second characteristic is that the *peak position* for the butterfly feature shifts negatively due to an increase of  $\Theta_{Pd}$ , by up to about 0.1 V from the position on bare Pt(111) to that on Pt(111) modified with a pseudomorphic Pd layer. This finding is consistent with the stronger affinity of Pd to oxygen [28, 29], as recently discussed for the oxide formation on Pt(111)-Pd in alkaline solution [17]. The third characteristic is that the charge associated with the “butterfly” formation decreases with increasing  $\Theta_{Pd}$  (see Figure 1c). Note, that the voltammograms of the palladium films illustrated in Figure 1 show some similarities and differences with the results recently presented by Alvarez et al. [27]. In agreement with reference [27] is the shape of the CV at low potentials and the integrated charge in the  $H_{upd}$  region. In the

OH adsorption potential region, however, there is no (small) sharp peak as reported in ref. [27]. The authors claim that this sharp peak is characteristic of highly-ordered Pt(111) substrates for the deposition, and does not occur on less well-ordered Pt(111) surfaces. The absence of this small peak in our voltammetry is probably indicative of the relative imperfection of our flame-annealed bulk single crystal versus the Clavilier “bead” single crystal employed in [27]. One aspect of the voltammetry not discussed in ref. [27], although it is present in their data as well as ours, is the decrease in total charge in OH adsorption region upon Pd deposition. This is a surprising result with respect to the greater oxophilicity of Pd. One possible explanation of this apparently conflicting behavior of palladium surface atoms (note, that there might be an electronic influence of the underlying platinum substrate) in  $\text{HClO}_4$  is the supposition that the adsorption of  $\text{OH}^-$  on the Pd sites is inhibited by the competitive adsorption of chloride anions. Small concentrations of chloride may be preexisting as a trace impurity even in “ultrapure”  $\text{HClO}_4$  and/or may be generated by the reduction of perchlorate ions catalyzed by palladium [32]. Consequently, the stronger Pd-Cl interaction (indicated by the higher bond energy in Pd-Cl than in Pt-Cl compounds [31]) may mean that  $\text{OH}_{\text{ad}}$  cannot displace all the  $\text{Cl}_{\text{ad}}$  from the surface, thereby leading to the “loss” of charge from ca.  $80 \mu\text{C}/\text{cm}^2$  on Pt(111) to ca.  $60 \mu\text{C}/\text{cm}^2$  on the Pt(111)-1 ML Pd surface in perchloric acid solution. At slow sweep rates (10 mV/s), the charge under the “butterfly” feature on the Pd covered Pt(111) surface decreases even further to ca.  $50 \mu\text{C}/\text{cm}^2$  whereas under identical experimental conditions the charge associated with the butterfly feature on bare Pt(111) remains unaffected.

In order to elucidate the possible role of very small amounts of chloride present in perchloric acid solution on the adsorption of  $H_{upd}$  and  $OH_{ad}$  on a Pt(111)-Pd electrode, in the present work the  $Cl^-$  concentration was intentionally increased in the vicinity of the electrode surface. In electrochemical experiments, the rate of mass transport of reactants to the electrode surface can usually be increased by the application of several methods, including the rotation of the electrode (or the stirring of the solution), a decrease of the sweep rate, an increase of the temperature, and an increase of the reactant concentration in the electrolyte. An enhanced mass-transport of the small amount of  $Cl^-$  (ca.  $10^{-7}$  M) from the bulk of “pure”  $HClO_4$  solution to the electrode surface by forced convection should have a similar effect as the addition of chloride to the electrolyte. Therefore in Figure 2 voltammetric profiles of the Pt(111)-Pd electrode in 0.1 M  $HClO_4$  and in 0.1 M  $HClO_4$  containing  $10^{-6}$  M  $Cl^-$  are presented with and without rotating the electrode. As can be seen in Figures 2c and d, the rotation of the electrode (1600 rpm) has a significant effect on both the shape of the  $H_{upd}$  peaks and on the adsorption of  $OH^-$ . In particular, the observed  $H_{upd}$  peaks in the voltammogram of the rotated electrode exhibit an asymmetry, in contrast to the relatively symmetrical  $H_{upd}$  peaks observed with a stationary electrode. This asymmetry displays the fact, that upon rotating the electrode the current density in the  $H_{upd}$  peak is increased in the cathodic sweep of the CV, whereas in the anodic sweep the observed current densities in the  $H_{upd}$  potential region are the same in the stationary experiments and under enhanced mass-transfer conditions. On the other hand in the  $OH^-$  adsorption potential region no peak can be observed anymore when rotating the electrode, indicating the complete blocking of the  $OH_{ad}$  adsorption by another species.

In the experiments presented in Figure 2b  $\text{Cl}^-$  is *intentionally* added to the solution. The observed voltammetric features in the presence of small amounts of chloride ( $10^{-6}$  M HCl) are qualitatively similar to the effect induced by a rotation of the electrode in “pure”  $\text{HClO}_4$ . Whereas the  $\text{H}_{\text{upd}}$  region in the anodic scan remains unaffected by the addition of small amounts of chloride, in the cathodic scan the various  $\text{H}_{\text{upd}}$  peaks merge into a single peak located at 0.2 V. Furthermore the  $\text{OH}^-$  adsorption is largely suppressed.

Interestingly, a very similar behavior is observed for the adsorption of hydrogen on Pt(100) in  $\text{HClO}_4$  containing  $5 \times 10^{-6}$  M  $\text{Cl}^-$  [32]. In order to explain the asymmetry of the  $\text{H}_{\text{upd}}$  peaks on Pt(100) in the presence of trace levels of  $\text{Cl}^-$ , the authors suggested that the diffusion controlled adsorption of  $\text{Cl}^-$  is responsible for the observed asymmetry. For details see reference [32]. Here the same reasoning is adopted and described in the following. We suggest, that the asymmetry of the  $\text{H}_{\text{upd}}$  peaks induced by the rotation of the Pt(111)-Pd electrode is due to an increased mass-transport of  $\text{Cl}^-$  from the bulk of the  $\text{HClO}_4$  solution to the electrode surface and due to an enhanced adsorption of  $\text{Cl}^-$  anions on the Pd sites. Consequently, the surface coverage of  $\text{Cl}_{\text{ad}}$  is higher on the RDE, resulting in an almost complete blocking of the  $\text{OH}^-$  adsorption. This leads to a shift of the  $\text{H}_{\text{upd}}$  peak, which follows the desorption of  $\text{Cl}_{\text{ad}}$ , to lower potentials when sweeping the potential from the positive limit to negative potentials, thereby producing a sharp peak located at ca. 0.2 V. After desorption,  $\text{Cl}^-$  diffuses away from the surface, and then re-adsorbs slowly in the positive sweep reaching the maximum surface coverage at the positive potential limit. The asymmetry observed in the  $\text{H}_{\text{upd}}$  potential region is, therefore, completely controlled by the different  $\text{Cl}_{\text{ad}}$  surface coverage in the positive and negative

sweep direction. Diffusion and  $H_{upd}$  desorption simultaneously control the  $Cl^-$  adsorption during the anodic sweep. Clearly, under enhanced mass-transfer conditions even traces of  $Cl^-$  present in ‘pure’  $HClO_4$  control completely the oxide formation on the Pt(111)-Pd surface. Therefore the observed effect of small amounts of chloride ( $10^{-6}$  M HCl), which are intentionally added to the solution (see Figure 2b), is qualitatively similar to the effect of rotation.

Very recently, it was shown that with an increased amount of chloride added to the perchloric acid ( $10^{-3}$  M HCl), the cyclic voltammogram of Pt(111)-1ML Pd becomes symmetrical again and simultaneous desorption/adsorption peaks can be seen in the anodic cycle of the  $H_{upd}$  potential region and vice versa in the cathodic cycle [33]. Notice that the same behavior was observed for the Pt(100)-Cl system in ref. [32] suggesting that trace amounts of  $Cl^-$  and *not* the high concentration of perchlorate anions control the adsorption properties of the Pt(111)-Pd surface. Although the binding energy of  $OH_{ad}$  is stronger on Pd than on Pt, due to the strong Pd-Cl interaction, the  $OH_{ad}$  coverage is higher on Pt(111) than on Pt(111)-1MLPd, a fact which will have consequences for our interpretation of the catalytic activity of Pt and Pd surfaces.

### 3.2 *In-situ* FTIR measurements

In our recent paper the electrooxidation of carbon monoxide on Pt(111)-xPd in alkaline solution was studied by FTIR spectroscopy [17]. The results clearly demonstrated that the kinetic rate of CO oxidation is inhibited on Pt(111) modified by Pd, despite of the fact that the adsorption of  $OH_{ad}$  is enhanced on Pd sites. As an explanation for these results we suggested that the kinetic rate of CO oxidation is strongly affected by

the delicate balance between the coverage and the nature of the electroactive species, the Pd-OH<sub>ad</sub> interaction being too strong to effectively oxidize adsorbed CO. In order to demonstrate that in acid solution competitive anion adsorption also plays a significant role in the kinetics of CO oxidation at the Pt(111)-xPd interfaces, the representative FTIR results for molecular level characterization of the surface chemistry of CO<sub>ad</sub> on the Pd modified Pt(111) surface in HClO<sub>4</sub> with and without Cl<sup>-</sup> are summarized in the Figures 3-6. When appropriate, these results will be compared with the corresponding results obtained in alkaline solutions.

In-situ FTIR measurements were performed on several thin palladium films with different Pd coverages supported on Pt(111). Figure 3 depicts potential dependent series of infrared spectra of CO adsorbed on three different Pt(111)-xPd surfaces in CO saturated perchloric acid solution. The reference spectra were recorded at 1.0 V. The behavior of CO<sub>ad</sub> on Pt(111) (x = 0, Figure 3a) is well known [34] and shall therefore be addressed first. At cathodic potentials below 0.6 V characteristic C-O stretching bands near 2070 and near 1790 cm<sup>-1</sup>, corresponding to CO adsorbed on atop- and three-fold hollow sites, respectively, can be distinguished. Going to more anodic potentials, the band of the hollow species is replaced by a new C-O stretching band at about 1840 cm<sup>-1</sup>, which can be related to the presence of bridge bonded CO. Comparison of the potential dependent intensity changes for the three-fold and bridge CO bands with surface X-ray scattering (SXS) data suggested that the three-fold hollow band (in combination with the on-top band) is related to a p(2 x 2)-3CO structure whereas the loss of this ordered structure is reflected by the appearance of the bridge-bonded CO band [34]. This change in the adsorption geometry is accompanied by the onset of CO<sub>ad</sub> oxidation (see CO<sub>2</sub>

production in unsaturated perchloric acid solution in Figure 4), which begins at a potential of about 0.55 V. As discussed in reference [34-36],  $\text{CO}_{\text{ad}}$  is oxidatively removed by reaction with  $\text{OH}_{\text{ad}}$  through a Langmuir-Hinshelwood mechanism.

For  $\text{Pt}(111)$  covered with a full monolayer of Pd FTIR spectra in CO saturated 0.1 M  $\text{HClO}_4$  (Figure 3c) reveal only one single absorption band near  $1920 \text{ cm}^{-1}$ . This finding is consistent with FTIR investigations of Inukai et al. [16] and Gil et al. [37] in sulfuric acid solution, where the absorption peak has been assigned to bridge-bonded  $\text{CO}_{\text{ad}}$ . In line with these studies, the band for  $\text{CO}_{\text{ad}}$  on 1 ML of Pd here also may be denoted as CO adsorbed at Pd bridge sites. Besides the major Pd- $\text{CO}_{\text{ad}}$  band also a small band at about  $2070 \text{ cm}^{-1}$  is present in the spectra. From Figure 3a it is clear that this band corresponds to the adsorption of CO on very *small* Pd-free platinum islands. Therefore, we conclude that the  $\text{Pt}(111)$  electrode is (almost completely) covered with a pseudomorphic palladium monolayer. The pseudomorphic growth of palladium on  $\text{Pt}(111)$  and its stability in acid [11] and alkaline solutions is confirmed by SXS measurements.

In Figure 3b a series of FTIR measurements of  $\text{CO}_{\text{ad}}$  on a  $\text{Pt}(111)$ -xML Pd electrode with  $x = 0.31$  can be seen. Even though FTIR spectra were recorded at surfaces modified by electrochemical Pd deposition in several submonolayer-to-monolayer quantities, this selected series of spectra is representative in order to demonstrate all important features of CO surface electrochemistry on a Pd modified  $\text{Pt}(111)$  surface in perchloric acid solution. At low potentials, three different C-O stretching bands near  $1800 \text{ cm}^{-1}$ ,  $1920 \text{ cm}^{-1}$  and  $2070 \text{ cm}^{-1}$  can be distinguished in the spectra. By comparison with Figures 3a and 3c, these bands can clearly be assigned to multi-coordinated CO

adsorbed on Pt, CO bridge-bonded on Pd and CO adsorbed a-top on Pt atoms, respectively. As discussed in previous work, the superposition of the Pt-CO and Pd-CO bands and the lack of a second Pd-CO band are indications for the growth of palladium islands of monoatomic height [16, 17].

As shown in the previous section, the effect of anions in the supporting electrolyte should also be taken into account when analyzing the CO oxidation reaction, i.e.,



While anions cannot compete with CO for the same adsorption sites, anions are always in strong competition with  $OH_{ad}$  adsorption. In Figure 4 we compare  $CO_2$  production on three different surfaces under the same experimental conditions. These measurements were recorded in argon-purged perchloric acid solution in order to prevent readsorption of CO from the electrolyte and to separate the amount of  $CO_2$  formed on the different surfaces more clearly. It can be seen that despite of the more or less same *onset potential* for the adsorption of OH species on Pt(111)-Pd and Pt(111) in the voltammograms (Figure 1) on a surface modified by Pd the onset of CO-oxidation is shifted to more positive potentials. This finding is in contrast to our results in alkaline solution, where the same onset of  $CO_2$  production was found for Pt(111) and Pt(111)-Pd [17]. Assuming that for the oxidation of  $CO_{ad}$  on Pt(111) and Pt(111)-Pd, respectively, the same Langmuir-Hinshelwood mechanism is active and bearing in mind that the formation of  $OH_{ad}$  starts at defect sites and steps on the surface [36], based on our voltammetric results it is reasonable to suggest that  $Cl^-$  can effectively suppress the onset potential and the rate of  $OH_{ad}$  formation, and thus the onset *and* the rate of CO oxidation ( $CO_2$  production in Figure 4).

For further support of the hypothesis of competitive anion adsorption, we compare the possible effects of  $\text{Cl}^-$  on the rate of CO oxidation ( $\text{CO}_2$  production) in  $\text{HClO}_4$  and  $\text{HClO}_4$  containing different amounts of  $\text{Cl}^-$  at the same pH of the solution. The corresponding FTIR results are shown in Figure 5 for CO adsorption on a  $\text{Pt}(111)\text{-xML Pd}$  electrode with  $x = 0.31$ . The measurements of Fig. 5 a are performed in perchloric acid whereas the spectra in Fig. 5b are recorded in the same solution containing  $10^{-2}$  M HCl, both solutions being CO saturated (the evaluated palladium coverage in Fig. 5 b is slightly different,  $x = 0.29$ ). Comparing the two series it is obvious that the chloride increases the stability of the  $\text{CO}_{\text{ad}}$  layer towards oxidation. Whereas in the chloride free electrolyte the CO adlayer is completely oxidized at 0.8 V, in the chloride containing electrolyte at 0.8 V both CO adsorbed on palladium and adsorbed on platinum can be detected. We sought to confirm the possible role of  $\text{Cl}^-$  anions by monitoring the  $\text{CO}_2$  production from solution containing different amounts of  $\text{Cl}^-$ . As depicted in Figure 6, increasing the Cl concentration, namely to  $10^{-4}$  M and  $10^{-2}$  M, respectively, shifts the onset potential for  $\text{CO}_2$  production to more positive potentials, is in line with the notion that Cl competes with  $\text{OH}_{\text{ad}}$  for the active sites. As a result, the kinetics of CO oxidation is hindered in the presence of  $\text{Cl}^-$  anions. The kinetics of the surface reaction given in Eq.1 is strongly affected by the delicate balance between the coverage of  $\text{CO}_{\text{ad}}$ ,  $\text{OH}_{\text{ad}}$  and anions, as discussed in our previous papers [20, 38-40].

#### 4. Conclusion

A combination of cyclic voltammetry and in-situ FTIR investigations has been used in order to describe the electrochemical behavior of thin palladium films supported on  $\text{Pt}(111)$  in perchloric acid solution. It has been shown that palladium affects the cyclic

voltammetry in perchloric acid in three characteristic ways. First of all, the hydrogen coverage in  $H_{upd}$  potential region is calculated to be 1ML, independent of the pH of the solution. This high coverage is attributed due to the strong interaction of Pd with hydrogen and/or the absence of lateral repulsion of the  $H_{upd}$ . Secondly, the onset potential for  $OH_{ad}$  formation is shifted to more negative potentials, but the charge density of the butterfly peak is considerably lower on Pt(111)-1MLPd than on bare Pt(111). The former is attributed to the greater oxophilicity of Pd vs. Pt, while the latter is attributed to competitive adsorption of chloride anions present as an impurity. This hypothesis is supported by additional experiments using intentionally added chloride.

The electrooxidation of  $CO_{ad}$  on Pt(111)-xPd films in perchloric acid solution is discussed in terms of the chloride impurity hypothesis. On the palladium films, the onset potential for oxidation is shifted towards more positive potentials. This apparently contradictory behavior is attributed to the effect of specific chloride adsorption on the formation of  $OH_{ad}$  on the Pd sites.

### **Acknowledgments**

This work was supported by the Director, Office of Science, Office of Basic Energy Sciences, Division of Materials Sciences, U.S. Department of Energy under Contract No. DE-AC03-76SF00098. M. A. acknowledges the German Academic Exchange Service (DAAD) for a scholarship.

## References

- [1] Rodriguez, J.A. and D.W. Goodman, *Science*, 1992. **257**(5072): p. 897-903.
- [2] Campbell, R.A., J.A. Rodriguez, and D.W. Goodman, *Physical Review B-Condensed Matter*, 1992. **46**(11): p. 7077-87.
- [3] Han, M., P. Mrozek, and A. Wieckowski, *Physical Review B-Condensed Matter*, 1993. **48**(11): p. 8329-8335.
- [4] Hammer, B., Y. Morikawa, and J.K. Norskov, *Physical Review Letters*, 1996. **76**(12): p. 2141-2144.
- [5] Mavrikakis, M., B. Hammer, and J.K. Norskov, *Physical Review Letters*, 1998. **81**(13): p. 2819-2822.
- [6] Pallassana, V., M. Neurock, L.B. Hansen, B. Hammer, and J.K. Norskov, *Physical Review B*, 1999. **60**(8): p. 6146-6154.
- [7] Attard, G. and A. Bannister, *Journal of Electroanalytical Chemistry*, 1991. **300**: p. 467.
- [8] Clavilier, J., M.J. Llorca, J.M. Feliu, and A. Aldaz, *Journal of Electroanalytical Chemistry*, 1991. **310**: p. 429.
- [9] Baldauf, M. and D.M. Kolb, *Journal of Physical Chemistry*, 1996. **100**(27): p. 11375-11381.
- [10] Climent, V., N.M. Markovic, and P.N. Ross, *Journal of Physical Chemistry B*, 2000. **104**(14): p. 3116-3120.
- [11] Markovic, N.M., C.A. Lucas, V. Climent, V. Stamenkovic, and P.N. Ross, *Surface Science*, 2000. **465**(1-2): p. 103-114.
- [12] Baldauf, M. and D.M. Kolb, *Electrochimica Acta*, 1993. **38**(15): p. 2145-2153.
- [13] Kibler, L.A., M. Kleinert, R. Randler, and D.M. Kolb, *Surface Science*, 1999. **443**(1-2): p. 19-30.
- [14] Naohara, H., S. Ye, and K. Uosaki, *Journal of Electroanalytical Chemistry*, 1999. **473**(1-2): p. 2-9.
- [15] Kibler, L.A., M. Kleinert, and D.M. Kolb, *Surface Science*, 2000. **461**(1-3): p. 155-167.
- [16] Inukai, J. and M. Ito, *Journal of Electroanalytical Chemistry*, 1993. **358**(1-2): p. 307-315.
- [17] Arenz, M., V. Stamenkovic, T.J. Schmidt, K. Wandelt, P.N. Ross, and N.M. Markovic, *Surface Science*, 2002. **506**(3): p. 287-296.
- [18] Ball, M., C.A. Lucas, N.M. Markovic, V. Stamenkovic, and P.N. Ross, submitted to *Surface Science*, 2002.
- [19] Paffett, M.T., C.T. Campbell, and T.N. Taylor, *Journal of Chemical Physics*, 1986. **85**(10): p. 6176-6185.
- [20] Markovic, N.M., C.A. Lucas, B.N. Grgur, and P.N. Ross, *Journal of Physical Chemistry B*, 1999. **103**(44): p. 9616-9623.
- [21] Markovic, N.M., H.A. Gasteiger, and P.N. Ross, *Journal of Physical Chemistry*, 1995. **99**(11): p. 3411-3415.
- [22] Markovic, N.M. and P.N. Ross, *Journal of Electroanalytical Chemistry*, 1992. **330**: p. 499.

- [23] Sawatari, Y., J. Inukai, and M. Ito, *Journal of Electron Spectroscopy & Related Phenomena*, 1993. **64-65**: p. 515.
- [24] Wagner, F.T. and P.N. Ross, *Journal of Electroanalytical Chemistry*, 1988. **250**: p. 301.
- [25] Markovic, N.M., T.J. Schmidt, B.N. Grgur, H.A. Gasteiger, R.J. Behm, and P.N. Ross, *Journal of Physical Chemistry B*, 1999. **103**(40): p. 8568-8577.
- [26] Koper, and M.T.M. Lukkien, J.J., *Journal of Electroanalytical Chemistry*, 2000. **485**: p. 161
- [27] Alvarez, B., J.M. Feliu, and Clavilier, J., *Electrochemistry Communications*, 2002. **4**: p. 379.
- [28] Tarasevich, B.J., D.A. Rand, and R. Woods, *Journal of Electroanalytical Chemistry*, 1973. **44**: p. 83.
- [29] Tarasevich, M.R., A. Sadkowski, and E. Yeager, *Oxygen Electrochemistry*, in *Comprehensive Treatise in Electrochemistry*, B.E. Conway, et al., Editors. 1983, Plenum Press: New York.
- [30] Kibler, L.A., private communication.
- [31] *CRC Handbook of Chemistry and Physics*. 66th ed, ed. R.C. Weast. 1986, Boca Raton, FL: CRC Press.
- [32] Markovic, N.M., M. Hanson, G. McDougall, and E. Yeager, *Journal of Electroanalytical Chemistry*, 1986. **214**: p. 555-566.
- [33] Schmidt, T.J., N.M. Markovic, V. Stamenkovic, P.N. Ross, G. Attard, and D. Watson, submitted to *Langmuir*, 2002.
- [34] Akemann, W., K.A. Friedrich, and U. Stimming, *Journal of Chemical Physics*, 2000. **113**(16): p. 6864-6874.
- [35] Lucas, C.A., N.M. Markovic, and P.N. Ross, *Surface Science*, 1999. **425**(1): p. L381-L386.
- [36] Lebedeva, N.P., M.T.M. Koper, J. Feliu, and R.A. v. Santen, *Journal of Electroanalytical Chemistry* (in press), 2002.
- [37] Gil, A., A. Clotet, J.M. Ricart, F. Illas, B. Alvarez, A. Rodes, and J.M. Feliu, *Journal of Physical Chemistry B*, 2001. **105**(30): p. 7263-7271.
- [38] Markovic, N.M., B.N. Grgur, C.A. Lucas, and P.N. Ross, *Surface Science*, 1997. **384**(1-3): p. L805-L814.
- [39] Markovic, N.M., B.N. Grgur, C.A. Lucas, and P.N. Ross, *Journal of Physical Chemistry B*, 1999. **103**(3): p. 487-495.
- [40] Markovic, N.M., C.A. Lucas, A. Rodes, V. Stamenkovic, and P.N. Ross, *Surface Science*, 2002. **499**: p. L149-L158.

## Figure Captions

**Figure 1:** a) Cyclic voltammograms of Pt(111)-xPd electrodes in 0.1 M HClO<sub>4</sub>; scan rate 50 mV/s at room temperature; the palladium coverage x increases from x = 0 to x = 0.15 and x = 1 (counted from top); b) CV H<sub>upd</sub> peak area versus palladium coverage; c) CV anodic peak area versus palladium coverage.

**Figure 2:** Cyclic voltammograms of Pt(111)-1ML Pd; scan rate 50 mV/s at room temperature; a) in 50 mM HClO<sub>4</sub>; b) in 0.1 M HClO<sub>4</sub> containing 10<sup>-6</sup> M HCl c) same conditions as in (a) but rotation of electrode with 1600 rpm; d) same conditions as in (b) but rotation of electrode with 1600 rpm.

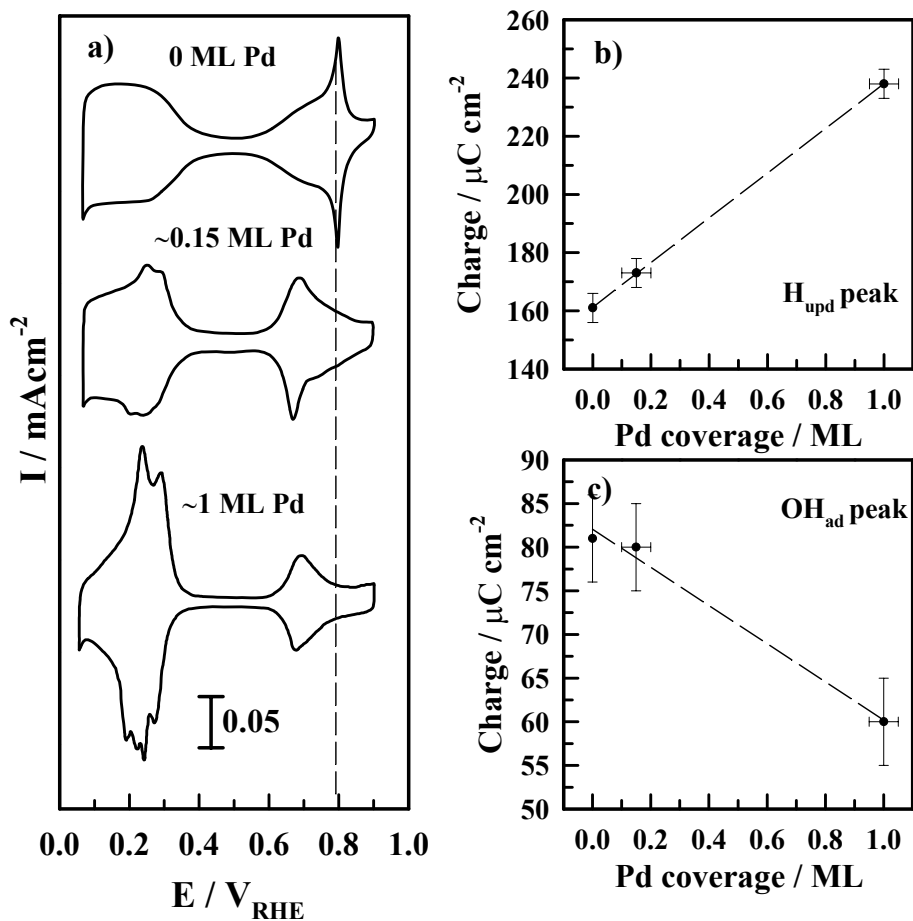
**Figure 3:** Series of infrared spectra of CO<sub>ad</sub> on (a) Pt(111), (b) Pt(111)-31%Pd and (c) Pt(111)-1MLPd obtained by stepping the applied potential in a positive direction in CO saturated 0.1 M HClO<sub>4</sub> solution; each spectrum was accumulated from 100 interferometer scans each the potential indicated; the reference potential was taken at 1.0 V vs. RHE.

**Figure 4:** CO<sub>2</sub> production from CO<sub>ad</sub> oxidation on three Pt(111)-xPd surfaces in argon purged perchloric acid solution as a function of the electrode potential, -0.05 V was used as reference potential.

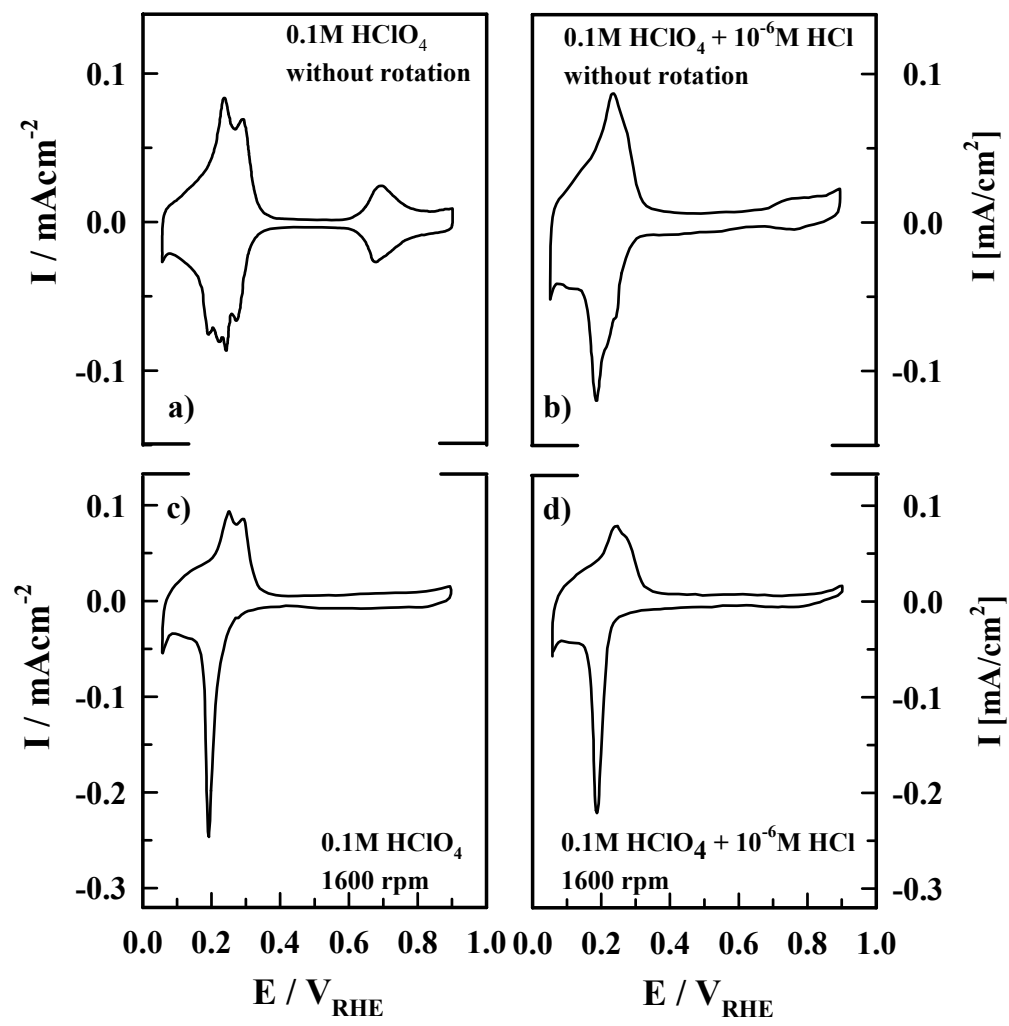
**Figure 5:** Series of infrared spectra of CO<sub>ad</sub> on Pt(111)-31%Pd in CO saturated 0.1 M HClO<sub>4</sub> solution; in (b) 10<sup>-2</sup> M HCl are added; each spectrum was accumulated from 100 interferometer scans at each potential indicated; the reference potential was 1.0 V vs. RHE.

**Figure 6:** Comparison of the CO<sub>2</sub> production as a function of Pd coverage.

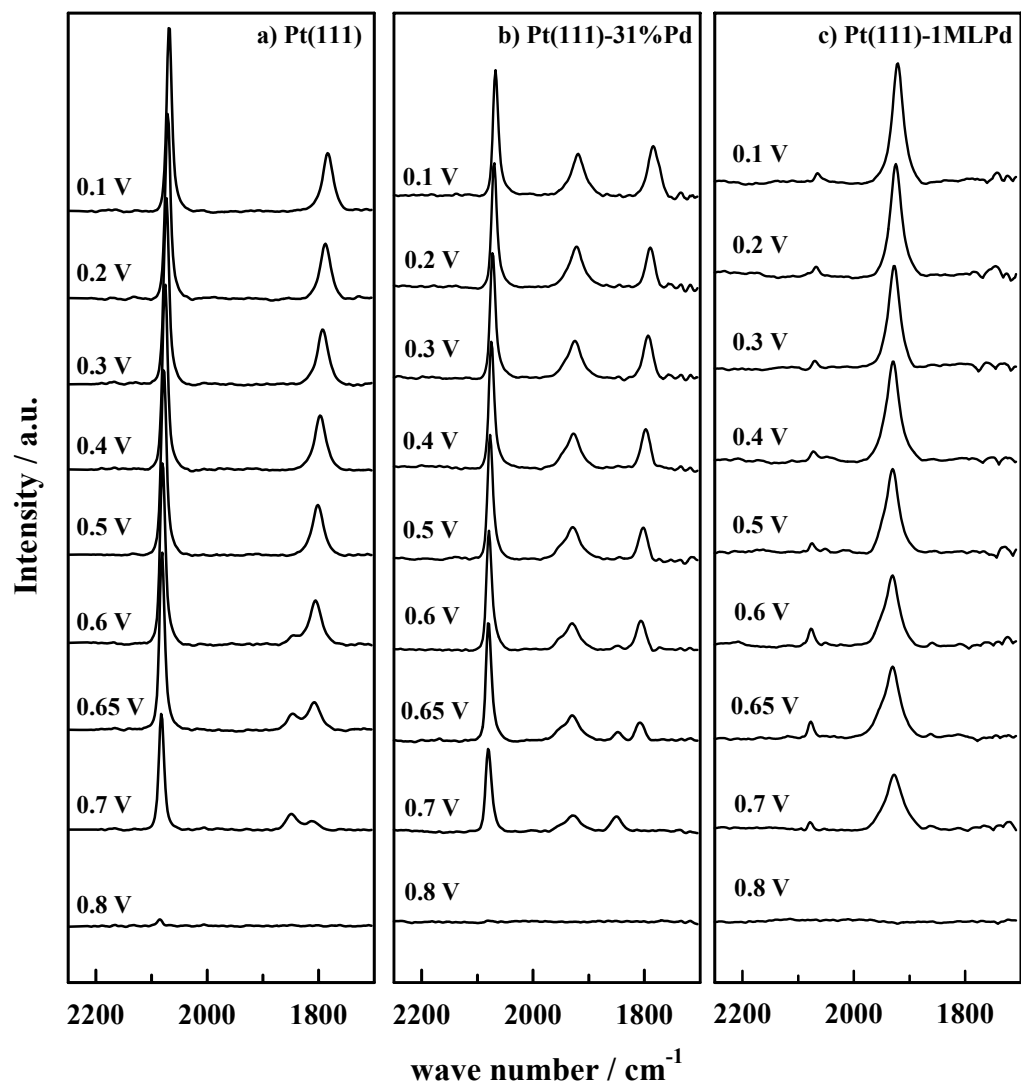




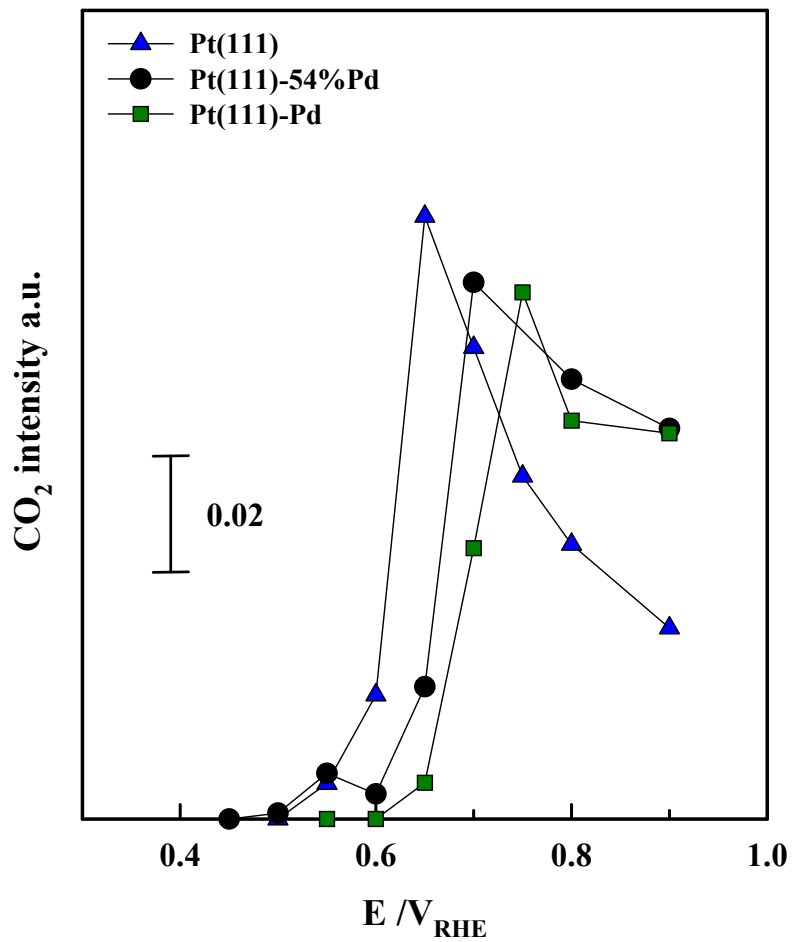
*Arenz et al. figure 1*



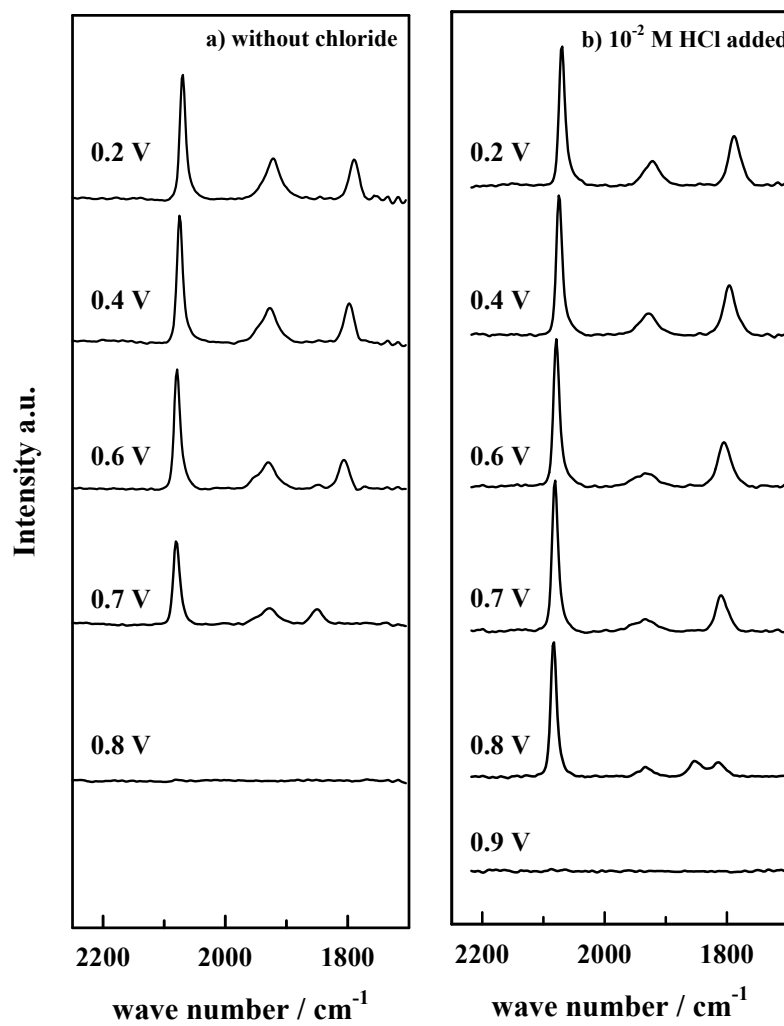
Arenz *et al.* figure 2



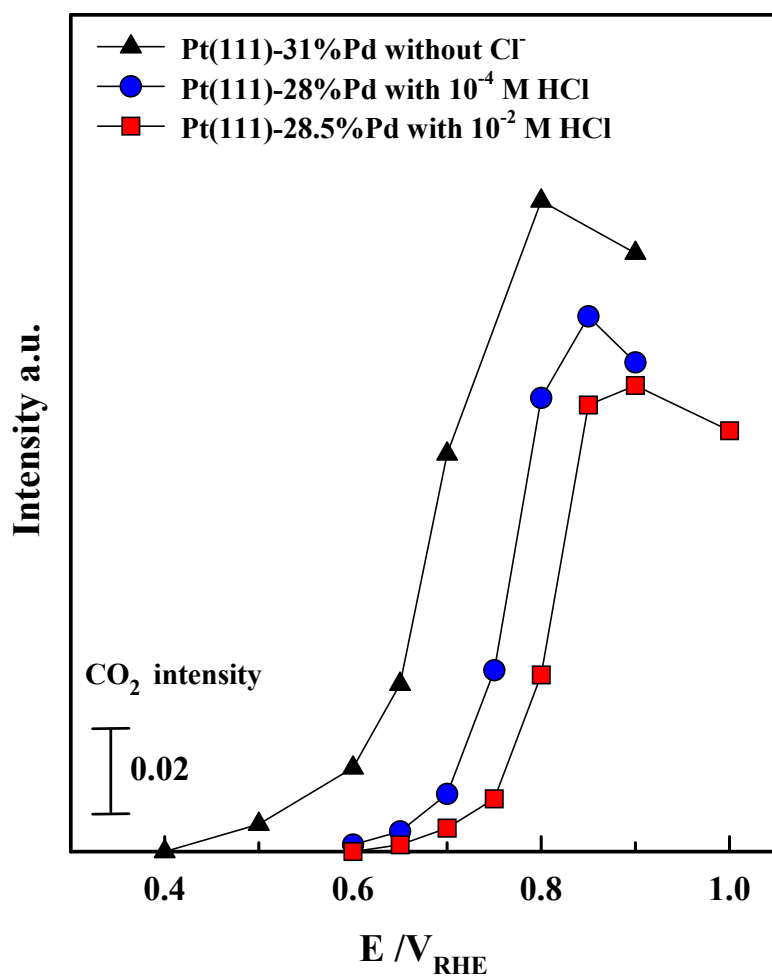
Arenz *et al.* figure 3



Arenz *et al.* figure 4



Arenz et al. figure 5



Arenz et al. figure 6